ISSN 0006-2979, Biochemistry (Moscow), 2014, Vol. 79, No. 2, pp. 102-110. © Pleiades Publishing, Ltd., 2014.
Published in Russian in Biokhimiya, 2014, Vol. 79, No. 2, pp. 144-153.
Originally published in Biochemistry (Moscow) On-Line Papers in Press, as Manuscript BM13-279, January 12, 2014.

ACCELERATED PUBLICATION

Pectin Methylesterase-Generated Methanol May Be Involved in Tobacco Leaf Growth

T. V. Komarova[1,2], D. V. Pozdyshev[1,2], I. V. Petrunia[2], E. V. Sheshukova[2], and Y. L. Dorokhov[1,2]*

[1]*Belozersky Institute of Physico-Chemical Biology, Lomonosov Moscow State University, 119991 Moscow, Russia; fax: +7 (495) 939-3181; E-mail: dorokhov@genebee.msu.su*
[2]*Vavilov Institute of General Genetics, Russian Academy of Sciences, ul. Gubkina 3, 119991 Moscow, Russia; fax: +7 (499) 132-8962; E-mail: dorokhov@genebee.msu.ru*

Received September 26, 2013
Revision received October 14, 2013

Abstract—Plant leaves undergo a sink–source modification of intercellular macromolecular transport during the transition from carbon import to carbon export. After assessing the role of metabolite signaling in gene regulation in *Nicotiana tabacum* sink and source leaves, we observed increased pectin methylesterase (PME)-mediated methanol generation in immature leaves. Using suppression subtractive hybridization (SSH), we identified a number of genes whose activity changes from sink to source leaves. The most abundant SSH-identified genes appeared to be sensitive to methanol. We hypothesize that tobacco leaf maturation and the sink–source transition are accompanied by a change in mRNA levels of genes that function in methanol-dependent cell signaling.

DOI: 10.1134/S0006297914020035

Key words: pectin methylesterase, methanol, movement, plasmodesmata, *Nicotiana tabacum*, transport

Plant growth and the transition from an immature apical leaf to a mature leaf are accompanied not only by an increase in cell size, but also by two important interconnected processes. First, there is a change in carbohydrate metabolism when immature leaves, which consume photosynthetic carbon (sink leaves), are converted into mature leaves (source leaves) [1]. During the second process, there is a modification of the intercellular transport of macromolecules carried out by plasmodesmata (PD) [2]. The sink leaf PD is simple and characterized by high capacity for providing free transport of macromolecules between cells, whereas the source leaf PD is branched, with limited macromolecular transport [2-5]. The sink–source transition occurs under strict genetic control and is very sensitive to signals far removed from the PD channel itself. For example, during the sink–source transition in *Arabidopsis thaliana*, *increased size exclusion limit 1* (*ISE1*) and *ISE2* [6-8] and *decreased size exclusion limit 1* (*DSE1*) [9] up- and down-regulate PD permeability, respectively. Cell expansion and maturation of the cell wall are also observed during the leaf sink–source transition. Because PD are imbedded in the cell wall, the changes in the cell wall during maturation affect the ability of the PD to increase or decrease their aperture size. Pectin methylesterase (PME) is an enzymatic factor involved in cell expansion and cell wall modification [10-12]. PME catalyzes the demethylesterification of pectin homogalacturonans by converting methoxyl groups into carboxyl groups, releasing both methanol and protons [13]. PME-generated methanol is therefore a byproduct of cell growth, and it is strongly correlated with cell and leaf expansion. Until recently, methanol was assumed to be a metabolic waste product of homogalacturonan demethylesterification. Leaf wounding results in enhanced methanol emission, which increases the accumulation of methanol-inducible gene (MIG) mRNAs and enhances antibacterial resistance, as well as cell–cell communication that facilitates viral spreading in neighboring plants [14]. Methanol probably functions as a signaling molecule that is important for intra- and inter-plant communication. However, there is also evidence for a potential role of methanol in the growth and development of plants [15].

In this study, we investigated whether methanol has a role as a signaling molecule involved in the growth and

Abbreviations: MIG, methanol-inducible gene; PD, plasmodesmata; PME, pectin methylesterase; SSH, suppression subtractive hybridization.

* To whom correspondence should be addressed.

development of plant leaves. We used tobacco (*Nicotiana tabacum*) leaves that, in contrast to other plants such as *Nicotiana benthamiana*, are well-studied with respect to the physiological and anatomical features of sink and source leaves [2-5]. We have identified novel methanol-inducible genes that are probably involved in regulation of the sink–source transformation of leaves.

MATERIALS AND METHODS

Plant growth conditions. *Nicotiana tabacum* cv. Samsun (nn) plants were grown in soil in a controlled environmental chamber with a 16 h/8 h day/night cycle and 25/18°C temperature. All plants used were 11-12-week-old and had five to six true leaves.

Methanol analysis. To analyze the methanol content in plant sap, 30 mg of leaf tissue was ground in the presence of Celite in microcentrifuge tubes and centrifuged at 16,000*g* for 10 min. An equal volume of 10% trichloroacetic acid was added to each supernatant aliquot. After 20 min incubation on ice, the samples were centrifuged at 16,000*g* for 15 min, and 2 μl of the supernatant was used for GC analysis as described previously [14].

Agroinjection experiments. *Agrobacterium tumefaciens* strain GV3101 was transformed with a binary vector encoding 2×GFP under control of cauliflower mosaic virus 35S promoter (CaMV 35S) and grown at 28°C in LB medium supplemented with 50 mg/liter rifampicin, 25 mg/liter gentamycin, and 50 mg/liter carbenicillin/kanamycin. *Agrobacterium* cells from an overnight culture (5 ml) were collected by centrifugation (10 min, 4500*g*), resuspended in 10 mM MES (pH 5.5) buffer supplemented with 10 mM $MgSO_4$, and adjusted to a final OD_{600} of 0.01. For cell-to-cell movement assays, *N. tabacum* plant leaves were agroinjected with CaMV 35S 2×GFP and stored for 24 h in a growth chamber at 24°C.

GFP detection. Fluorescent cells containing 2×GFP were counted using an Axiovert 200M fluorescence microscope and the following set of filters: BP470/40 (excitation) and BP525/50 (emission) (Zeiss, Germany).

Suppression subtractive hybridization (SSH). Total RNA was isolated from 3-cm sink and 10-13-cm source tobacco leaves. Amplified double-stranded cDNA was prepared from sink and source leaf RNA with oligonucleotide and CDS primers using the SMART approach [16]. The subtraction was performed in two directions: sink leaf cDNA library was subtracted from source leaf cDNA, and vice versa (http://evrogen.ru/services/cDNA-subtraction/service-cdna-subtraction.shtml).

q-PCR analysis of transcript levels. Total RNA was extracted from plant tissues using TriReagent (MRC, USA) according to the manufacturer's protocol. After DNase treatment (Fermentas, Lithuania), 2 μg of denatured total RNA was annealed with 0.1 μg of random hexamers and 0.1 μg of Oligo-dT, followed by incubation with 200 units of Superscript II reverse transcriptase (Invitrogen, USA) for 50 min at 43°C to generate cDNA. Real-time qPCR was carried out using an iCycler iQ Real Time PCR detection system (Bio-Rad, USA) as described previously [14]. The thermal profile for EVA Green real-time qPCR included an initial heat-denaturing step at 95°C for 3 min followed by 45 cycles with a denaturation step at 95°C for 15 s, an annealing step for 30 s, and an elongation step at 72°C for 30 s, coupled with measurement of fluorescence. The target gene mRNA levels were normalized to the corresponding reference genes (*N. tabacum* 18S RNA). The following primers were used: "BG-F1" GATTGTTGTGTCCGAGAGTG; "BG-R1" CCAGTTCAGGGTTCTTGTTG; "NCAPP-F1" CTATGTCTTCAAAGATTAGTCTG; "NCAPP-R1" GGACGGAAATGATTGTGGC; "PME-F1" ATCCTTGGATTCCGGCAAGAACGT; "PME-R1" AAACACTTGCAATTGTAGAGTAAC; "PI-II-F1" ATGTACCTCGCCAAACTTAC; "PI-II-R1" CTCCATCTATTTATAGCAAACG; "MIG-21-F1" AGGAAGGCAGTTTCATGCATAA; "MIG-21-R1" GCCTCTTATTTGTTTGAGTTATGCCTC; "ISE2-F1" ACAGTGGCAAAAGGAAGG; "ISE2-R1" TAAGAGGAGTAGTATAGAATAGTC; "ERP-F1" TGATGGTGGCTATGGTAGTG; "ERP-R1" CTGGCTCTGGCTGTAGTG; "SEO-F1" CTGGAAGCATTGGAAGAGAAGG; "SEO-R1" GGTTGTGAGCGAGTGAAGC; "SABC-F1" TGTCCCTGGTCTTTACTATTCG; "SABC-R1" GCGGTGATTATTGTGATGAGC; "ARP-F1" GGATGATGTTATGGCTGGAC; "ARP-R1" GTGACGGAGTTGTTGGTG; "ST-F1" TCAAGACCAACACTACACTCC; and "ST-R1" CCACCCACCACTGATAATAGG.

Whole plant methanol treatment. Plants were treated with methanol by exposing them to methanol vapors in a single hermetically-sealed 20-liter desiccator. Pots (width, 9.5 cm; depth, 9.5 cm) containing plants (10.0 ± 1.0 g) and soil (198.0 ± 20.0 g) were placed into desiccators with methanol (160 mg) applied to filter paper as described previously [14], and then maintained for 3 h at constant temperature of 24°C. The final concentration of gaseous methanol was 17.5 μg per gram leaf fresh weight. The treated plants were withdrawn from the desiccator, and leaf RNA was isolated as described above.

RESULTS

Measurements of PME mRNA and methanol accumulation in tobacco sink and source leaves. We studied the role of PME in the sink–source transition using young tobacco (*N. tabacum* cv. Samsun nn) plants with 5-6 true leaves (Fig. 1a). For young immature expanding sink leaves, we used small leaves that were 3 cm in length (Fig. 1a, top inset). We chose leaves that were 10-13 cm in

length (Fig. 1a, bottom inset) located in the lower tiers of the tobacco plant as mature source leaves. An important characteristic of sink leaves is that dilated PD are open to the movement of protein molecules as large as 47 kDa [3]. To evaluate cell-to-cell communication in sink and source leaves, a reporter macromolecule was used to test movement through PD in different states of dilation. We chose a reporter containing two fused copies of green fluorescent protein (2×GFP). We exploited a previously described "agroinjection strategy" to deliver the CaMV 35S 2×GFP containing plasmid into the cell [14]. To monitor single infection sites, the tobacco plants were agroinjected with a diluted (OD_{600} ~ 0.01) bacterial suspension, and fluorescent cells were counted after 24 h of incubation in a growth chamber at 24°C. Counting the number of epidermal cells that displayed fluorescence provides a quantitative measure of 2×GFP movement. When the PD were closed, 2×GFP was detected mainly in single cells (Fig. 1b, upper). However, fluorescence signals were distributed in 2- or 4-cell clusters (Fig. 1b, bottom) when the PD were dilated. In the source leaves approximately 15% of the signal was distributed in 2- to 4-cell clusters, whereas in sink leaves approximately 25% of the signal was distributed in 2- to 4-cell clusters (Fig. 1c), thus indicating that the ability to support cell-to-cell movement of 2×GFP was enhanced in sink leaves. An unpaired two-tailed Student's *t*-test confirmed the statistical significance of the differences in the cell-to-cell movement of 2×GFP between the source and sink leaves.

To study leaf PME synthesis, we analyzed PME mRNA content in immature and mature tobacco leaves by quantitative real-time PCR. We found that immature leaves have more than twice greater level of PME mRNA compared to mature tobacco leaves (Fig. 1d). We next expected to observe higher methanol levels in the sap of immature leaves as a result of PME activity. We observed an almost two-fold decrease in methanol in the leaf sap of mature leaves compared to immature leaves (Fig. 1e).

The mRNA accumulation levels in mature and immature leaves were then analyzed for the following genes previously identified as being sensitive to gaseous methanol and involved in plant immunity: *β-1,3-glucanase* (*BG*), *methanol inducible gene 21* (*MIG-21*), *non-cell-autonomous pathway protein* (*NCAPP*), and *proteinase inhibitor II* (*PI-II*) [14]. Although *NCAPP* mRNA levels were approximately equal in mature and immature leaves, the expression of *BG*, *MIG-21*, and *PI-II* increased significantly during leaf maturation (Table 1). In accordance with a previous study [8], we observed a decrease in *ISE2* mRNA expression in mature leaves.

Thus, we conclude that the sink–source transition is accompanied by two events. First, there is a change in the transcriptional activity of stress genes, as shown by a decrease in the level of PME mRNA accumulation and an increase in MIG (BG, MIG-21, and PI-II) mRNA levels in source leaf. The second event observed is a reduction in the concentration of methanol in source leaf sap, which correlates with a decrease in the transcriptional activity of *PME*.

Identification of genes involved in growth and development of tobacco leaves and their sensitivity to methanol. To better understand the mechanisms of gene regulation involved in the sink–source transition, we created a cDNA library from sink and source tobacco leaves and analyzed them using SSH. We identified a total of 92 differentially expressed transcripts, 26 of which were enriched mainly in source leaves and 66 of which were primarily expressed in sink leaves (Table 2).

We selected a few genes to further analyze based on the following properties: first, we selected genes that were represented with a large number of clones in the SSH analysis and second, we selected genes with possible functions in leaf growth and development and/or in the sink–source transformation. We selected five genes: *sugar transporter* (*ST*) [17, 18], *auxin-repressed protein* (*ARP*) [19], *elicitor responsible protein* (*ERP*) [20], *salicylic acid binding catalase* (*SABC*) [21, 22], and *sieve element occlusion protein* (*SEOP*) [18, 22, 23], the putative functions of which are described in Table 2.

We next validated the changes in gene expression observed by SSH by performing qRT-PCR to determine the mRNA levels in sink and source leaves. We found that

Table 1. Relative quantity of *MIGs* and *ISE2* mRNAs in *N. tabacum* leaves

Tobacco leaves	Relative quantity of mRNA*				
	BG ($P < 0.001$)	*NCAPP* (**)	*MIG-21* ($P < 0.001$)	*PI-II* ($P < 0.001$)	*ISE2* ($P < 0.05$)
Sink (3 cm)	0.83 ± 0.08	0.80 ± 0.10	0.98 ± 0.03	1.01 ± 0.02	1.00 ± 0.10
Source (10-13 cm)	41.29 ± 1.61	1.14 ± 0.14	21.85 ± 3.30	3.87 ± 0.28	0.76 ± 0.05

* The data shown represent five independent experiments. The standard errors and the unpaired two-tailed Student's *t*-test *P*-values for the statistical significance of the difference between the sink and source leaves are indicated.

** n.s., not significantly different (Student's *t*-test).

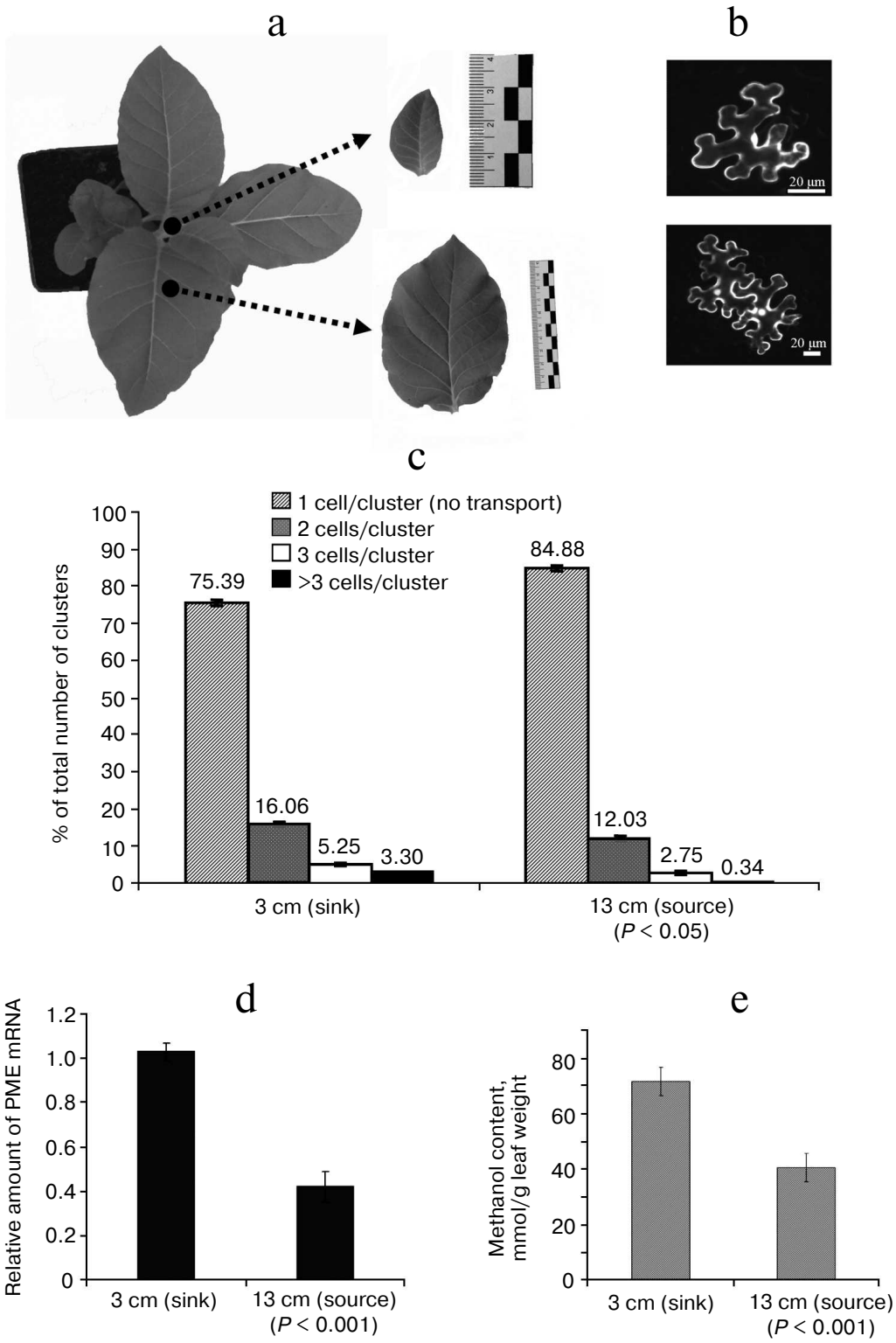

Fig. 1. *PME* mRNA levels and methanol accumulation are increased in tobacco sink leaves. a) A standard *Nicotiana tabacum* cv. Samsun (nn) plant and the detached sink (upper) and source (bottom) leaves used for analysis. b) Single (upper) and multiple (bottom) epidermal cells containing 2×GFP were observed in sink and source leaves using epifluorescence microscopy. c) Quantification of 2×GFP movement in sink and source leaves. No fewer than 1000 cell clusters were counted for each experiment. The data shown represent five independent experiments. Standard error bars are indicated. The *P*-value from an unpaired two-tailed Student's *t*-test is indicated. d) The relative levels of *PME* mRNA in sink and source leaves were determined by qRT-PCR. The data represent five independent experiments. Standard error bars and the *P*-value (unpaired two-tailed Student's *t*-test) are indicated. e) Methanol content in the sap of sink and source leaves. Error bars indicate the standard error of the data from six independent samples. The *P*-value from an unpaired two-tailed Student's *t*-test is indicated.

Table 2. List of *Nicotiana tabacum* expressed sequence tags (ESTs) identified by SSH

Gene	Functional annotation	Matching with		EST clones (number)	European Nucleotide Archive accession number
		species	*E*-value		
1	2	3	4	5	6
		Upregulated in source leaves			
*Sugar transporter (*ST*)	Putative SWEET-like bidirectional sugar transporter involved in movement of photoassimilates and the sink–source transition [17, 18]	*S. lycopersicum*	1e-29 1e-29 7e-149 7e-149 5e-171	5	HG425058 HG425064 HG424987 HG425059 HG425069
*Auxin-repressed protein (*ARP*)	Genetic target of auxins regulating plant growth, translation [19]	*N. tabacum*	8e-54 0 0	3	HG425066 HG425070 HG425074
*Elicitor responsible protein (ERP)	Photoassimilates and viruses phloem transport [20], protein glycosylation	*N. tabacum*	5e-105 0 0	3	HG424989 HG424990 HG424991
	Uncharacterized cDNA, unknown function	*S. lycopersicum*	3e-84 9e-105	2	HG425057 HG424988
		No homologues found		2	HG425055 HG425063
Glucosyltransferase	Sugars biosynthesis	*N. tabacum*	8e-172	1	HG425054
Glutathione transferase	Detoxification	*N. benthamiana*	1e-152	1	HG425060
*Salicylic acid binding catalase (*SABC*)	Salicylic acid binding protein, taking part in plant growth [21] and protecting cells from the toxic effects of hydrogen peroxide	*N. tabacum*	0	1	HG425067
GRP3	Glycine-rich protein precursor	*N. tabacum*	0	1	HG425056
ATP carrier protein	ADP/ATP translocase	*S. tuberosum*	0	1	HG425071
ATOX1-like	Putative copper transport protein	*S. lycopersicum*	3e-109	1	HG425073
Putative peptide/ /nitrate transporter At5g14940-like	Putative peptide/nitrate transporter	*S. lycopersicum*	1e-162	1	HG425068
Putative chloroplast thiazole biosynthetic protein	Putative chloroplast thiazole biosynthetic protein	*N. tabacum*	1e-161	1	HG425062
Putative elongation factor Tu, mitochondrial-like	Elongation of translation	*S. lycopersicum*	0	1	HG425072
	Uncharacterized cDNA, unknown function	*S. lycopersicum*	7e-115	1	HG425061
	Uncharacterized cDNA, unknown function	*S. lycopersicum*	6e-16	1	HG425065
		Upregulated in sink leaves			
Chlorophyll a/b binding proteins (*CABs*)	Photosynthesis	*N. tabacum*	0	11	HG424982

Table 2. (Contd.)

1	2	3	4	5	6
			3e-96		HG424994
			0		HG425000
			0		HG425003
			0		HG425010
			0		HG425018
			0		HG425019
			0		HG425032
			7e-97		HG425042
			0		HG425048
			8e-119		HG425005
Chloroplast genome encoded ribosomal proteins	Chloroplast protein biosynthesis	*N. tabacum*	0	8	HG424986
			0		HG425013
			0		HG425014
			0		HG425030
			0		HG425034
			0		HG425045
			0		HG425049
			5e-97		HG425031
*Sieve element occlusion protein (*SEOP*)	Transport of photoassimilates, phloem sieve elements reparation [18, 22, 23]	*N. tabacum*	0	4	HG425012
			0		HG425008
			0		HG425021
			0		HG425022
H2A and H3 histone proteins	Histones	*N. tabacum*	0	4	HG424983
			0		HG425011
			5e-159		HG425017
			0		HG425023
		No homologues found		4	HG424985
					HG425006
					HG425024
					HG425043
Oxygen evolving complex 33 kDa photosystem II protein	Photosynthesis	*N. tabacum*	0	3	HG425001
			3e-178		HG425036
			0		HG425037
Chloroplast plastocyanin precursor	Photosynthesis	*N. benthamiana*	3e-154	3	HG425007
			0		HG425020
			5e-126		HG425044
Mg protoporphyrin IX chelatase	Protoporphyrin biosynthesis	*N. tabacum*	0	2	HG424999
			0		HG425038
NADPH:protochlorophyllide oxidoreductase	Porphyrin and chlorophyll biosynthesis	*N. tabacum*	3e-136	2	HG424993
			0		HG425029
Plasma membrane intrinsic protein *PIP2*	Signal transduction	*S. chacoense*	3e-168	2	HG424995
			8e-60		HG425028
Ascorbate oxidase-related protein	Ascorbate metabolism	*N. tabacum*	0	2	HG425027
			3e-166		HG425051
Lipase At5g33370-like	Lipid metabolism	*S. lycopersicum*	5e-36	2	HG424984
			2e-76		HG425047
Maturase K	tRNA maturation	*N. tabacum*	0	1	HG425025
Chloroplast genome encoded tRNA	tRNA biosynthesis	*N. tabacum*	0	1	HG425035

Table 2. (Contd.)

1	2	3	4	5	6
RNA binding protein	Protein biosynthesis	*N. plumbaginifolia*	0	1	HG424997
Chloroplast carbonic anhydrase	Photosynthesis	*N. tabacum*	0	1	HG425039
Putative porphobilinogen deaminase, chloroplastic-like	Porphyrin and chlorophyll biosynthesis	*S. lycopersicum*	0	1	HG424992
Putative cytochrome P450 77A3-like	Cytochrome family member	*S. lycopersicum*	0	1	HG424998
Putative pentatricopeptide repeat-containing protein At1g74850, chloroplastic-like	Transcription regulation	*S. lycopersicum*	0	1	HG425041
Acyl carrier protein	Lipid biosynthesis and metabolism	*S. lycopersicum*	6e-91	1	HG425002
1-deoxy-D-xylulose-5-phosphate synthase	Steroid biosynthesis	*N. tabacum*	0	1	HG425009
Cellulose synthase catalytic subunit	Cellulose biosynthesis	*N. alata*	0	1	HG425040
Leucine rich repeat receptor protein kinase (*CLAVATA1*)	Morphogenesis	*S. peruvianum*	0	1	HG425015
ROX1 homolog	Hypersensitive response	*N. tabacum*	0	1	HG425033
Guard cell proline-rich protein	Guard cell protein	*S. tuberosum*	0	1	HG425052
Serine hydroxymethyltransferase 1-like	Amino acids metabolism	*S. lycopersicum*	0	1	HG425016
Putative early nodulin-like protein 2-like	Signal transduction, stress-induced protein	*S. lycopersicum*	4e-137	1	HG425004
Putative polygalacturonase At1g48100-like	Cell wall metabolism	*S. lycopersicum*	0	1	HG424996
Putative T-complex protein 1 subunit theta-like	Chaperone-like protein	*S. lycopersicum*	0	1	HG425046
	Uncharacterized cDNA, unknown function	*N. tabacum*	0	1	HG425050
	Uncharacterized cDNA, unknown function	*S. lycopersicum*	2e-115	1	HG425053

* Genes selected for further analysis.

leaf maturation was accompanied by an accumulation of *ST*, *ARP*, *ERP*, and *SABC* mRNA and a decrease in *SEOP* mRNA levels (Fig. 2a).

The ability of the selected genes to alter their activity under the influence of methanol was tested. We observed an abrupt and significant accumulation of *SEOP*, *ARP*, and *SABC* mRNA when leaves were exposed to gaseous methanol (Fig. 2b).

We hypothesize that the methanol generated by PME can function as a transcriptional regulator of gene activity during the sink–source transition.

DISCUSSION

Until recently, methanol was considered to be a metabolic product of PME activity during growth and cell wall modification [10, 11]. Recent data suggest a role for gaseous methanol in intra- and inter-plant communication [14]. Here we demonstrated that the methanol content in the sap of immature leaves is elevated compared to levels in mature leaves (Fig. 1e). We believe that the methanol detected in each leaf was synthesized by the cells of the individual leaf and not introduced by the

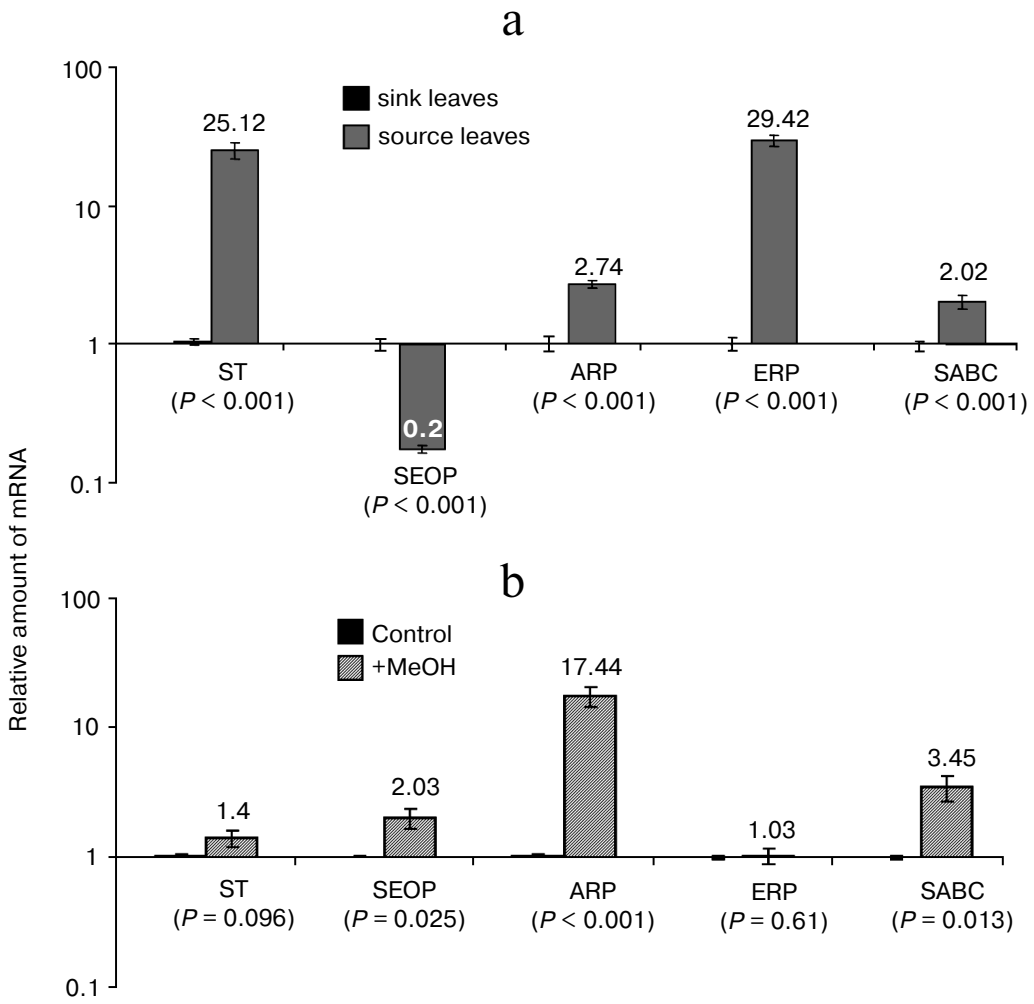

Fig. 2. Analysis of mRNA selected by SSH. a) Verification of genes identified by SSH in the cDNA libraries from tobacco leaves. The semi-log plot shows the relative levels of *ST*, *SEOP*, *ARP*, *ERP*, and *SABC* mRNA isolated from sink and source leaves. b) Relative levels of *ST*, *SEOP*, *ARP*, *ERP*, and *SABC* mRNA in *N. tabacum* leaves after methanol treatment. The data shown represent five independent experiments. The standard error bars and the *P*-value (unpaired two-tailed Student's *t*-test) are indicated.

phloem sap from other parts of the plant for several reasons. First, the rate of methanol emission (i.e. release of methanol into the air) is correlated with the age of the leaf. Isolated immature leaves emit substantially greater amounts of gaseous methanol than mature leaves [15]. Second, underground methanol production is not essential to the level and emission of methanol in mature and immature leaves [24]. Finally, according to our data, the methanol concentration is correlated with cellular PME mRNA levels in mature and immature leaves (Fig. 1, d and e).

Synthesis of PME is one of the factors in plant growth, leading to pectin demethylation, which accompanies the natural division and maturation of the plant cell. In general, homogalacturonan demethylesterification catalyzed by PME is likely to be a module of plant cell growth control, providing constant remodeling and modification after deposition of the homogalacturonans [25]. Interestingly, overexpression of PME in transgenic plants leads to increased levels of aberrant synthesis of methanol [14], which is accompanied by dwarfism of tobacco [26].

The conversion of homogalacturonan methoxyl groups into carboxyl groups results in methanol release. Methanol is not toxic to plant cells, but rather performs an alarm function and is able to control the activity of genes involved in intercellular transport [14]. Immature leaves are characterized by intense intercellular transport of macromolecules. The PD play an important role in this process, and in immature leaves they are regulated in turn by metabolic signals, among which methanol may be one of the key players. To experimentally confirm this proposed relationship, we have identified mRNAs that differ significantly between mature and immature leaves (Table

2). Two genes, *ST* [17, 18] and *SEOP* [18, 22, 23], are directly involved with the operation of phloem transport of carbohydrates in plants, and *ARP* [19], ERP [20] and *SABC* [21] are involved in plant morphogenesis and cell signaling. Among the genes identified, at least three (*SEOP*, *ARP*, and *SABC*) are sensitive to methanol (Fig. 2b).

The mechanism of methanol effect on genes involved in sink-source transition remains unclear, but the transcriptional activity of these genes is apparently affected by the specific microenvironment and the concentration of methanol generated during the cell wall modification process.

This work was supported by grants (Nos. 11-04-01152 and 12-04-33016) from the Russian Foundation for Basic Research (to T.V.K.) and stipend of the President of the Russian Federation for young scientists (to T.V.K.).

REFERENCES

1. Ayre, B. G. **(**2011) *Mol. Plant.*, **4**, 377-394.
2. Burch-Smith, T. M., and Zambryski, P. C. (2012) *Annu. Rev. Plant. Biol.*, **63**, 239-260.
3. Oparka, K. J., Roberts, A. G., Boevink, P., Santa Cruz, S., Roberts, I., Pradel, K. S., Imlau, A., Kotlizky, G., Sauer, N., and Epel, B. (1999) *Cell*, **97**, 743-754.
4. Crawford, K., and Zambryski, P. (2000) *Curr. Biol.*, **10**, 1032-1040.
5. Crawford, K., and Zambryski, P. C. (2001) *Plant Physiol.*, **125**, 1802-1812.
6. Burch-Smith, T. M., Brunkard, J. O., Choi, Y. G., and Zambryski, P. C. (2011) *Proc. Natl. Acad. Sci. USA*, **108**, E1451-1460.
7. Burch-Smith, T. M., Stonebloom, S., Xu, M., and Zambryski, P. C. (2011) *Protoplasma*, **248**, 61-74.
8. Burch-Smith, T. M., and Zambryski, P. C. (2010) *Curr. Biol.*, **20**, 989-993.
9. Xu, M., Cho, E., Burch-Smith, T. M., and Zambryski, P. C. (2012) *Proc. Natl. Acad. Sci. USA*, **109**, 5098-5103.
10. Micheli, F. (2001) *Trends Plant. Sci.*, **6**, 414-419.
11. Pelloux, J., Rusterucci, C., and Mellerowicz, E. J. (2007) *Trends Plant. Sci.*, **12**, 267-277.
12. Markovic, O., and Janecek, S. (2004) *Carbohydrate Res.*, **339**, 2281-2295.
13. Nemecek-Marshall, M., MacDonald, R. C., Franzen, J. J., Wojciechowski, C. L., and Fall, R. (1995) *Plant Physiol.*, **108**, 1359-1368.
14. Dorokhov, Y. L., Komarova, T. V., Petrunia, I. V., Frolova, O. Y., Pozdyshev, D. V., and Gleba, Y. Y. (2012) *PLoS Pathog.*, **8**, e1002640.
15. Huve, K., Christ, M. M., Kleist, E., Uerlings, R., Niinemets, U., Walter, A., and Wildt, J. (2007) *J. Exp. Bot.*, **58**, 1783-1793.
16. Diachenko, L., Lau, Y. F., Campbell, A. P., Chenchik, A., Mogadam, F., Huang, B., Lukyanov, S., Lukyanov, K., Gurskaya, N., Sverdlov, E. D., and Siebert, D. (1996) *Proc. Natl. Acad. Sci. USA*, **93**, 6025-6030.
17. Chen, L. Q., Qu, X. Q., Hou, B. H., Sosso, D., Osorio, S., Fernie, A. R., and Frommer, W. B. (2012) *Science*, **335**, 207-211.
18. Bihmidine, S., Hunter, C. T., 3rd, Johns, C. E., Koch, K. E., and Braun, D. M. (2013) *Front. Plant Sci.*, **4**, 177.
19. Li, Y., Wu, M. Y., Song, H. H., Hu, X., and Qiu, B. S. (2005) *Arch. Virol.*, **150**, 1993-2008.
20. Chen, Z., Silva, H., and Klessig, D. F. (1993) *Science*, **262**, 1883-1886.
21. Sanchez-Casas, P., and Klessig, D. F. (1994) *Plant Physiol.*, **106**, 1675-1679.
22. Ernst, A. M. (2012) *Proc. Natl. Acad. Sci. USA*, **109**, E1980-1989.
23. Lee, J., Han, C. T., and Hur, Y. (2013) *Mol. Biol. Rep.*, **40**, 197-209.
24. Oikawa, P. Y., Giebel, B. M., Sternberg, L., Li, L., Timko, M. P., Swart, P. K., Riemer, D. D., Mak, J. E., and Lerdau, M. T. (2011) *New Phytol.*, **191**, 1031-1040.
25. Wolf, S., and Greiner, S. (2012) *Protoplasma*, **249**, Suppl. 2, S169-175.
26. Hasunuma, T., Fukusaki, E., and Kobayashi, A. (2004) *J. Biotechnol.*, **111**, 241-251.